

Chiral 3π -exchange NN-potentials: Results for dominant next-to-leading order contributions

N. Kaiser

Physik Department T39, Technische Universität München,
D-85747 Garching, Germany

Abstract

We calculate in (two-loop) chiral perturbation theory the local NN-potentials generated by the three-pion exchange diagrams with one insertion from the second order chiral effective pion-nucleon Lagrangian proportional to the low-energy constants $c_{1,2,3,4}$. The resulting isoscalar central potential vanishes identically. In most cases these 3π -exchange potentials are larger than the ones generated by the diagrams involving only leading order vertices due to the large values of $c_{3,4}$ (which mainly represent virtual Δ -excitation). A similar feature has been observed for the chiral 2π -exchange. We also give suitable (double-integral) representations for the spin-spin and tensor potentials generated by the leading-order diagrams proportional to g_A^6 involving four nucleon propagators. In these cases the Cutkosky rule cannot be used to calculate the spectral-functions in the infinite nucleon mass limit since the corresponding mass-spectra start with a non-vanishing value at the 3π -threshold. Altogether, one finds that chiral 3π -exchange leads to small corrections in the region $r \geq 1.4$ fm where 1π - and chiral 2π -exchange alone provide a very good strong NN-force as shown in a recent analysis of the low-energy pp-scattering data-base.

PACS: 12.20.Ds, 12.38.Bx, 12.39.Fe, 13.75.Cs.

To be published in *The Physical Review C* (2000)

Over the last years effective field theory methods have been successfully applied to the two-nucleon system at low and intermediate energies [1, 2, 3, 4, 5, 6, 7]. The idea of constructing the NN-potential from effective field theory was put forward by Weinberg [1] and this was taken up by van Kolck and collaborators [2]. Their NN-potential contained one- and two-pion exchange graphs based on time-ordered perturbation theory (regularized by a Gaussian cut-off) and a host of contact interactions. The method of unitary transformations was used by Epelbaum, Glöckle and Meißner [4] to construct an energy-independent NN-potential from the effective chiral pion-nucleon Lagrangian. Based on one- and two-pion exchange and a few contact interactions which contribute only to S- and P-waves a good description of the deuteron properties as well as the NN phase-shifts and mixing angles below $T_{lab} = 300$ MeV was found in that framework [5].

The issue of the chiral 3π -exchange was first addressed by Pupin and Robilotta [8] who considered one particularly simple diagram with no internal nucleon propagators. In a recent work [9] we have started to calculate the static NN-potentials generated by the (two-loop) 3π -exchange diagrams with all possible interaction vertices taken from the leading-order effective chiral πN -Lagrangian. In ref.[9] we restricted ourselves to the evaluation of four relatively simple classes of diagrams with the common prefactor g_A^2/f_π^6 . It was stressed in ref.[9] that the chiral $3\pi NN$ -contact vertex employed in ref.[8] depends on the choice of the interpolating pion-field and therefore one has to consider representation invariant classes of diagrams by supplementing graphs involving the chiral 4π -vertex. Another obvious consequence of this

is that there is no unique definition of the so-called "pion-nucleon form factor" which is often introduced in phenomenological models. The only meaningful separation of the NN-potential is the one into point-like 1π -exchange and 3π -exchange. The four classes of 3π -exchange diagrams evaluated in ref.[9] gave rise only to isovector spin-spin and tensor potentials with a strength of ± 0.1 MeV or less at $r = 1.0$ fm. Compared to the chiral 2π -exchange NN-potentials [6, 7] these are negligibly small corrections.

In a subsequent work [10] the static NN-potentials generated by the 3π -exchange diagrams proportional to g_A^4 and g_A^6 (grouped into classes V, VI, VII, VIII and IX) have been worked out. The resulting coordinate space potentials have typical strengths of a few MeV at $r = 1.0$ fm. A surprising result of ref.[10] was that the total isoscalar central 3π -exchange NN-potential vanishes identically. The static 3π -exchange NN-potentials have been constructed in refs.[9, 10] from the mass-spectra (i.e. the imaginary parts) of the respective two-loop diagrams in the infinite nucleon mass limit $M \rightarrow \infty$. This method could however not be successfully applied to the spin-spin and tensor potentials generated by the diagrams proportional to g_A^6 (classes VIII and IX) involving four nucleon propagators. In these cases the integrand of the 3π -phase space integral $\int \int_{z^2 < 1} d\omega_1 d\omega_2 \dots$ developed a non-integrable singularity of the form $(1 - z^2)^{-3/2}$ on the boundary $z^2 = 1$. By considering the analytically solvable example of the crossed three-boson exchange with scalar coupling in ref.[10] the failure of the spectral-function method could be understood from the fact that in the limit $M \rightarrow \infty$ the mass-spectrum starts with a non-vanishing value at the 3-boson threshold $\mu = 3m$. In coordinate space this feature manifests itself as a large- r asymptotics of the form $e^{-3mr} r^{-2}$.

The purpose of this work is to present suitable double-integral representations for these remaining 3π -exchange spin-spin and tensor NN-potentials proportional to g_A^6 together with numerical results. Furthermore, will work out here the next-to-leading order corrections to the chiral 3π -exchange NN-potential. In general, the next-to-leading order contributions are given by all diagrams with one insertion from the second order chiral πN -Lagrangian $\mathcal{L}_{\pi N}^{(2)}$. However, from an analogous calculation of the chiral 2π -exchange in ref.[6] one has experienced that the dominant contributions come from the second order chiral $\pi\pi NN$ -contact vertex proportional to the low-energy constants $c_{1,2,3,4}$, whereas the relativistic $1/M$ -corrections are much smaller. The exception to this is, of course, the spin-orbit NN-potential which is a truly relativistic effect vanishing in the infinite nucleon mass limit $M \rightarrow \infty$. Therefore we will consider here only the two-loop 3π -exchange diagrams with exactly one insertion proportional to $c_{1,2,3,4}$. The corresponding effective chiral πN -Lagrangian reads

$$\mathcal{L}_{\pi N}^{(2)} = \bar{N} \left\{ 2c_1 m_\pi^2 (U + U^\dagger) + c_2 u_0^2 + c_3 u_\nu u^\nu + \frac{i}{2} c_4 \vec{\sigma} \cdot (\vec{u} \times \vec{u}) \right\} N, \quad (1)$$

with the axial vector quantity $u^\nu = i\{\xi^\dagger, \partial^\nu \xi\}$. The unitary matrix $\xi^2 = U = 1 + i\vec{\tau} \cdot \vec{\pi}/f_\pi - \vec{\pi}^2/2f_\pi^2 + \dots$ collects the Goldstone pion-fields and $f_\pi = 92.4$ MeV denotes the weak pion decay constant. The low-energy constants $c_{1,2,3,4}$ have been determined in a one-loop chiral perturbation theory analysis of low-energy πN -scattering in the physical region [11] and inside the Mandelstam triangle [12]. Their central values are $c_1 = -0.8 \text{ GeV}^{-1}$, $c_2 = 3.2 \text{ GeV}^{-1}$, $c_3 = -4.7 \text{ GeV}^{-1}$ and $c_4 = 3.4 \text{ GeV}^{-1}$. We prefer to use the values obtained in ref.[12] since at the small sub-threshold pion-energies relevant inside the Mandelstam triangle the chiral expansion of the πN -scattering amplitude is expected to work best. As outlined in ref.[13] the large low-energy constants $c_{2,3,4}$ receive dominant contributions from virtual $\Delta(1232)$ -isobar excitation. In ref.[7] it has been demonstrated that the 2π -exchange NN-potentials generated by explicit $\Delta(1232)$ -isobar excitation are very similar to those obtained from the $NN\pi\pi$ -contact interaction [6] proportional to $c_{1,2,3,4}$. In the so-called small scale expansion of ref.[14] the ΔN mass-splitting $\Delta = 293$ MeV is treated as a further small expansion parameter and 2π -exchange graphs with Δ -excitation are counted as leading order ones. This is another reason to focus

on the 3π -exchange potential proportional to $c_{1,2,3,4}$. The second order chiral $\pi\pi NN$ -contact vertex following from eq.(1) reads

$$\frac{i}{f_\pi^2} \left\{ -2\delta^{ab} [2c_1 m_\pi^2 + c_2 q_a^0 q_b^0 + c_3 q_a \cdot q_b] + c_4 \epsilon^{abc} \tau^c \vec{\sigma} \cdot (\vec{q}_a \times \vec{q}_b) \right\}, \quad (2)$$

where both pion four-momenta q_a and q_b are out-going ones. Note that the isoscalar part in eq.(2) is spin-independent while the isovector part is spin-dependent.

Next, let us give some basic definitions in order to fix our notation. In the static limit and considering only irreducible diagrams the on-shell NN T-matrix takes the following form

$$\begin{aligned} \mathcal{T}_{NN} = & V_C(q) + V_S(q) \vec{\sigma}_1 \cdot \vec{\sigma}_2 + V_T(q) \vec{\sigma}_1 \cdot \vec{q} \vec{\sigma}_2 \cdot \vec{q} \\ & + [W_C(q) + W_S(q) \vec{\sigma}_1 \cdot \vec{\sigma}_2 + W_T(q) \vec{\sigma}_1 \cdot \vec{q} \vec{\sigma}_2 \cdot \vec{q}] \vec{\tau}_1 \cdot \vec{\tau}_2, \end{aligned} \quad (3)$$

where $q = |\vec{q}|$ denotes the momentum transfer between the initial and final-state nucleon. The subscripts C, S and T refer to the central, spin-spin and tensor components, each of which occurs in an isoscalar ($V_{C,S,T}$) and an isovector version ($W_{C,S,T}$). As indicated, the (real) NN-amplitudes $V_C(q), \dots, W_T(q)$ depend only on the momentum transfer q in the static limit $M \rightarrow \infty$. We are here interested only in the coordinate-space potentials generated by certain diagrams in which three pions are simultaneously exchanged between both nucleons. For this purpose it is sufficient to calculate the imaginary parts of the NN-amplitudes, $\text{Im} V_{C,S,T}(i\mu)$ and $\text{Im} W_{C,S,T}(i\mu)$, analytically continued to time-like momentum transfer $q = i\mu - 0^+$ with $\mu \geq 3m_\pi$. These imaginary parts are then the mass-spectra entering a representation of the local coordinate-space potentials in the form of a continuous superposition of Yukawa-functions,

$$\tilde{V}_C(r) = -\frac{1}{2\pi^2 r} \int_{3m_\pi}^{\infty} d\mu \mu e^{-\mu r} \text{Im} V_C(i\mu), \quad (4)$$

$$\tilde{V}_S(r) = \frac{1}{6\pi^2 r} \int_{3m_\pi}^{\infty} d\mu \mu e^{-\mu r} [\mu^2 \text{Im} V_T(i\mu) - 3 \text{Im} V_S(i\mu)], \quad (5)$$

$$\tilde{V}_T(r) = \frac{1}{6\pi^2 r^3} \int_{3m_\pi}^{\infty} d\mu \mu e^{-\mu r} (3 + 3\mu r + \mu^2 r^2) \text{Im} V_T(i\mu). \quad (6)$$

The isoscalar central, spin-spin and tensor potentials, denoted here by $\tilde{V}_{C,S,T}(r)$, are as usual those ones which are accompanied by the operators $1, \vec{\sigma}_1 \cdot \vec{\sigma}_2$ and $3 \vec{\sigma}_1 \cdot \hat{r} \vec{\sigma}_2 \cdot \hat{r} - \vec{\sigma}_1 \cdot \vec{\sigma}_2$, respectively. For the isovector potentials $\tilde{W}_{C,S,T}(r)$ a completely analogous representation holds. The imaginary parts entering eqs.(4,5,6) are calculated from the pertinent 2-loop 3π -exchange diagrams as integrals of the $\bar{N}N \rightarrow 3\pi \rightarrow \bar{N}N$ transition amplitudes over the Lorentz-invariant 3π -phase space making use of the Cutkosky cutting rule as explained in refs.[9, 10, 15]. The sub-leading 3π -exchange considered here occurs at fifth order in small momentum (or chiral) expansion. Of course at this order there are also many two-loop 2π -exchange diagrams proportional to $c_{1,2,3,4}$. Since the corresponding spectral-functions will (in general) contain one-loop sub-divergences (related to the fourth order chiral πN -amplitude) an adequate discussion of these 2π -exchange potentials requires good knowledge of the strength of the counter-terms \bar{e}_i in $\mathcal{L}_{\pi N}^{(4)}$ [16]. With these included the corresponding 2π -exchange potential is well-defined, however, its explicit computation goes far beyond the scope of the present paper.

We start with the diagrams of class X shown in Fig.1. The heavy dot symbolizes the second order chiral $\pi\pi NN$ -contact vertex eq.(2) proportional to $c_{1,2,3,4}$. Diagrams for which the role of both nucleons is interchanged are not shown. These lead to the same contribution to the NN-potential, i.e. a factor of 2. As stressed in ref.[9] diagrams involving the chiral $3\pi NN$ -vertex or the chiral 4π -vertex depend on an arbitrary parameter and therefore one should consider the full class X as one entity. Obviously, the last two pion-pole diagrams in Fig.1 contribute via coupling constant renormalization also to the point-like 1π -exchange. This effect is however automatically taken care by working with the physical (on-shell) πNN -coupling constant $g_{\pi N}$.

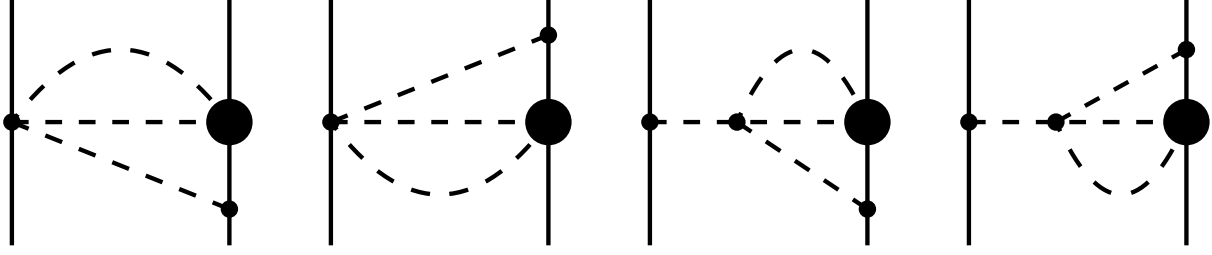


Fig.1: 3π -exchange diagrams of class X proportional to g_A^2 . Solid and dashed lines represent nucleons and pions, respectively. The heavy dot symbolized an insertion from second order chiral πN -Lagrangian. The combinatoric factor of these diagrams is $1/2$. Diagrams for which the role of both nucleons is interchanged are not shown. They lead to the same NN-potential.

Note that we are considering here only the finite-range Yukawa-parts of the 1π -exchange and we disregard all zero-range $\delta^3(\vec{r})$ -terms. Transformed into momentum space the latter become polynomials in q^2 with possible contributions from higher-derivative operators. From an inspection of the spin- and isospin factors occurring in the diagrams of class X one finds immediately that only non-vanishing isovector spin-spin and tensor NN-amplitudes $W_{S,T}$ will be obtained. We find the following imaginary parts from class X (dropping from now on the argument $i\mu$),

$$\begin{aligned} \text{Im } W_S^{(X)} &= \frac{g_A^2}{(4f_\pi)^6 \pi^2 \mu^3} \int_{2m_\pi}^{\mu - m_\pi} dw \sqrt{w^2 - 4m_\pi^2} \left\{ [2C_{13}(w) + \frac{c_2}{3}(w^2 - 4m_\pi^2)] \lambda(w) \right. \\ &\quad \left. + \frac{c_4}{3}(w^2 - 4m_\pi^2) [(w^2 - m_\pi^2)^2 + \mu^2(2m_\pi^2 + 2w^2 - 3\mu^2)] \right\}, \end{aligned} \quad (7)$$

$$\begin{aligned} \text{Im } W_T^{(X)} &= \frac{1}{\mu^2} \text{Im } W_S^{(X)} + \frac{g_A^2}{(4f_\pi)^6 \pi^2 \mu^5} \int_{2m_\pi}^{\mu - m_\pi} dw \sqrt{w^2 - 4m_\pi^2} \left\{ [4C_{13}(w) + \frac{2c_2}{3}(w^2 - 4m_\pi^2)] \right. \\ &\quad \times (\mu^2 + m_\pi^2 - w^2) [\mu^2 + m_\pi^2 - w^2 + 2\mu^2(2w^2 - \mu^2)(\mu^2 - m_\pi^2)^{-1}] \\ &\quad \left. + \frac{2c_4}{3}(w^2 - 4m_\pi^2) \lambda(w) (m_\pi^2 + 3\mu^2)(m_\pi^2 - \mu^2)^{-1} \right\}, \end{aligned} \quad (8)$$

where we have introduced the abbreviations $C_{13}(w) = 4c_1 m_\pi^2 + c_3(w^2 - 2m_\pi^2)$ and $\lambda(w) = w^4 + \mu^4 + m_\pi^4 - 2w^2 \mu^2 - 2w^2 m_\pi^2 - 2\mu^2 m_\pi^2$. The variable w denotes the invariant mass of a pion-pair and its kinematically allowed range is $2m_\pi \leq w \leq \mu - m_\pi$. The dw -integrals in eqs.(7,8) could of course be solved easily in terms of square-root and logarithmic functions. However, we want to avoid the resulting rather lengthy expressions.

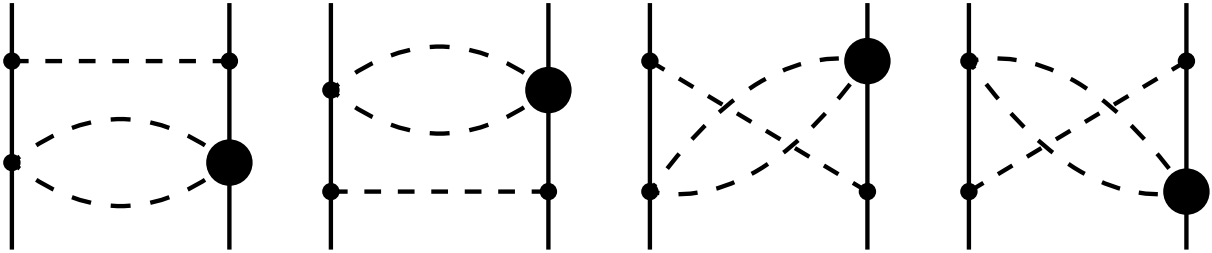


Fig.2: 3π -exchange diagrams of class XI proportional to g_A^2 . These give a vanishing contribution to the NN-potential.

Next, we consider the diagrams of class XI shown in Fig.2. Each of them gives a vanishing contribution to the NN T-matrix for the following reason. Since the leading order (Weinberg-Tomozawa) $\pi\pi NN$ -vertex is of isovector nature (i.e. proportional to $\epsilon^{abc} \tau^c$) a non-zero isospin-factor is obtained only from the spin-dependent isovector term in eq.(2) proportional to c_4 .

When combined with the spin-independent Weinberg-Tomozawa vertex on the other side of the bubble-type sub-diagram one finds immediately that the pertinent 1-loop integral is zero in the heavy baryon formalism (basically because the spin-vector $\vec{\sigma}$ has no time-component).

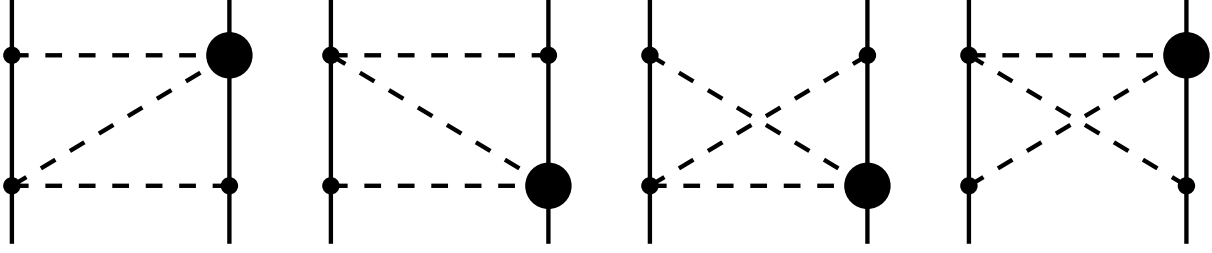


Fig.3: 3π -exchange diagrams of class XII proportional to g_A^2 . For further notation, see Fig. 1.

Next, we consider the diagrams of class XII shown in Fig.3. The isoscalar contribution comes exclusively from the c_4 -term in eq.(2). Altogether one obtains the following imaginary parts of the isoscalar and isovector spin-spin and tensor NN-amplitudes from class XII,

$$\text{Im } V_S^{(XII)} = \frac{2g_A^2 c_4}{(4f_\pi)^6 \pi^2 \mu^3} \int_{2m_\pi}^{\mu-m_\pi} dw \sqrt{w^2 - 4m_\pi^2} \lambda(w) [7m_\pi^2 - \mu^2 - 3w^2 + 2m_\pi^2(m_\pi^2 - \mu^2)w^{-2}], \quad (9)$$

$$\begin{aligned} \text{Im } V_T^{(XII)} &= \frac{1}{\mu^2} \text{Im } V_S^{(XII)} + \frac{4g_A^2 c_4}{(4f_\pi)^6 \pi^2 \mu^5} \int_{2m_\pi}^{\mu-m_\pi} dw \sqrt{w^2 - 4m_\pi^2} (\mu^2 + m_\pi^2 - w^2) \\ &\quad \times [3w^4 - 2w^2(5m_\pi^2 + 2\mu^2) + \mu^4 + 2\mu^2 m_\pi^2 + 5m_\pi^4 + 2m_\pi^2(\mu^2 - m_\pi^2)^2 w^{-2}], \end{aligned} \quad (10)$$

$$\begin{aligned} \text{Im } W_S^{(XII)} &= \frac{g_A^2}{(4f_\pi)^6 \pi^2 \mu^3} \int_{2m_\pi}^{\mu-m_\pi} dw \sqrt{w^2 - 4m_\pi^2} \left\{ [2C_{13}(w) + \frac{c_2}{3}(w^2 - 4m_\pi^2)] \lambda(w) \right. \\ &\quad \left. + \frac{c_4}{3}(w^2 - 4m_\pi^2) [(\mu^2 - m_\pi^2)(3\mu^2 + m_\pi^2 - 2w^2) - w^4] \right\}, \end{aligned} \quad (11)$$

$$\begin{aligned} \text{Im } W_T^{(XII)} &= \frac{1}{\mu^2} \text{Im } W_S^{(XII)} + \frac{g_A^2}{(4f_\pi)^6 \pi^2 \mu^5} \int_{2m_\pi}^{\mu-m_\pi} dw \sqrt{w^2 - 4m_\pi^2} \left\{ [(w^2 - m_\pi^2)^2 - \mu^4] \right. \\ &\quad \left. \times [4C_{13}(w) + \frac{2c_2}{3}(w^2 - 4m_\pi^2)] - \frac{2c_4}{3}(w^2 - 4m_\pi^2) \lambda(w) \right\}. \end{aligned} \quad (12)$$

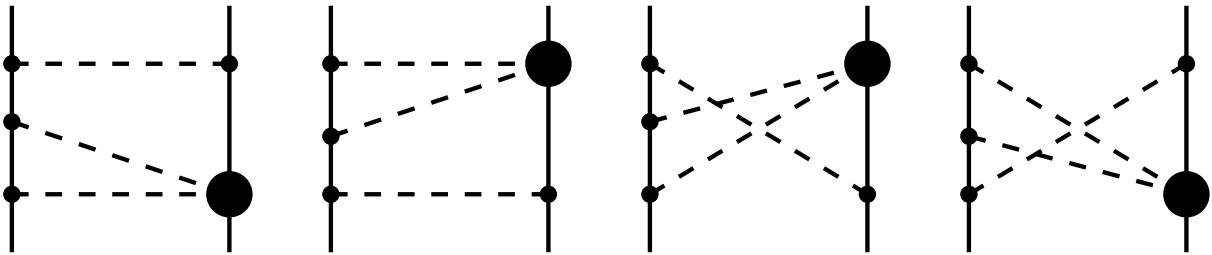


Fig.4: 3π -exchange diagrams of class XIII proportional to g_A^4 . For further notation, see Fig. 1.

Next, we turn to the diagrams of class XIII shown in Fig.4. The technique to separate off the iterative part from the first two reducible diagrams has been explained in ref.[10]. The iterative (or reducible) part is defined here (entirely) within perturbation theory as that part which carries in the numerator the large scale enhancement factor M , the nucleon mass. Such an

iterative part does therefore not obey the naive chiral power counting rules (see also section 4.3 in ref.[6] on the so-called iterated 1π -exchange). A detailed discussion of possible ambiguities showing up in (non-perturbative) iterations to infinite orders (e.g. via a Schrödinger equation) can be found in ref.[17]. The isovectorial spin-dependent contact vertex proportional to c_4 (and in fact only this one) produces now also a central NN-amplitude. Interestingly, its isoscalar and isovector components come with a fixed ratio. The corresponding imaginary parts read

$$\text{Im } V_C^{(XIII)} = -\frac{3}{4} \text{Im } W_C^{(XIII)} = \frac{12g_A^4 c_4}{(4f_\pi)^6 \pi^2 \mu} \int_{2m_\pi}^{\mu-m_\pi} dw \sqrt{w^2 - 4m_\pi^2} \lambda(w). \quad (13)$$

Furthermore, the isoscalar and isovector spin-spin and tensor NN-amplitudes generated by the diagrams of class XIII have the following imaginary parts,

$$\begin{aligned} \text{Im } V_S^{(XIII)} &= \frac{g_A^4 c_4}{(4f_\pi)^6 \pi^2 \mu^3} \int_{2m_\pi}^{\mu-m_\pi} dw \sqrt{w^2 - 4m_\pi^2} \left\{ 7\mu^6 - 37\mu^4 m_\pi^2 + 45\mu^2 m_\pi^4 - 15m_\pi^6 + 9w^6 \right. \\ &\quad \left. - w^4(11\mu^2 + 37m_\pi^2) + w^2(45m_\pi^4 + 32\mu^2 m_\pi^2 - 5\mu^4) + 2m_\pi^2(\mu^2 - m_\pi^2)^3 w^{-2} \right\} \end{aligned} \quad (14)$$

$$\begin{aligned} \text{Im } V_T^{(XIII)} &= \frac{1}{\mu^2} \text{Im } V_S^{(XIII)} + \frac{2g_A^4 c_4}{(4f_\pi)^6 \pi^2 \mu^5} \int_{2m_\pi}^{\mu-m_\pi} dw \sqrt{w^2 - 4m_\pi^2} \\ &\quad \times \left\{ 9w^6 - w^4(19\mu^2 + 37m_\pi^2) + w^2(11\mu^4 + 52\mu^2 m_\pi^2 + 45m_\pi^4) \right. \\ &\quad \left. - \mu^6 - 13\mu^4 m_\pi^2 - 35\mu^2 m_\pi^4 - 15m_\pi^6 + 2m_\pi^2(m_\pi^2 - \mu^2)(\mu^4 - m_\pi^4)w^{-2} \right\}, \end{aligned} \quad (15)$$

$$\begin{aligned} \text{Im } W_S^{(XIII)} &= \frac{g_A^4}{(4f_\pi)^6 \pi^2 \mu^3} \int_{2m_\pi}^{\mu-m_\pi} dw \sqrt{w^2 - 4m_\pi^2} \left\{ 3C_{13}(w) [4\mu^2(\mu^2 - m_\pi^2 - w^2) - \lambda(w)] \right. \\ &\quad \left. + \frac{c_2}{2}(8m_\pi^2 - 5w^2)\lambda(w) + 4c_4 [w^6 - w^4(\mu^2 + 4m_\pi^2) \right. \\ &\quad \left. + w^2(\mu^4 - 2\mu^2 m_\pi^2 + 5m_\pi^4) - \mu^6 + 4\mu^4 m_\pi^2 - \mu^2 m_\pi^4 - 2m_\pi^6] \right\}, \end{aligned} \quad (16)$$

$$\begin{aligned} \text{Im } W_T^{(XIII)} &= \frac{1}{\mu^2} \text{Im } W_S^{(XIII)} + \frac{g_A^4}{(4f_\pi)^6 \pi^2 \mu^5} \int_{2m_\pi}^{\mu-m_\pi} dw \sqrt{w^2 - 4m_\pi^2} \left\{ (m_\pi^2 + \mu^2 - w^2) \right. \\ &\quad \times [6C_{13}(w)(3\mu^2 + w^2 - m_\pi^2) + c_2(8m_\pi^2 - 5w^2)(m_\pi^2 + \mu^2 - w^2)] \\ &\quad \left. + 8c_4(w^2 - 2m_\pi^2)[(w^2 - m_\pi^2)^2 - \mu^4] \right\}. \end{aligned} \quad (17)$$

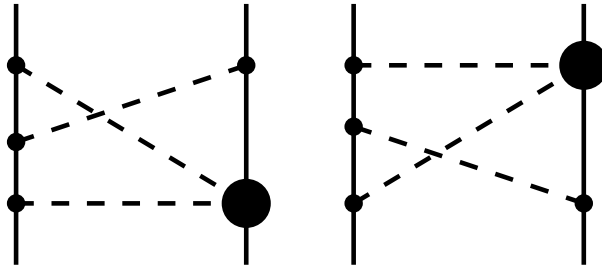


Fig.5: 3π -exchange diagrams of class XIV proportional to g_A^4 . For further notation, see Fig. 1.

Finally, we consider the (irreducible) diagrams of class XIV shown in Fig.5. In this case the isovectorial c_4 -term in eq.(2) does not make a contribution to the isovector NN-amplitudes

$W_{C,S,T}$. One obtains from class XIV an isoscalar central NN-amplitude which is however exactly canceled by the one coming from class XIII,

$$\text{Im } V_C^{(XIV)} = -\text{Im } V_C^{(XIII)}. \quad (18)$$

Therefore, one has the interesting result that there is no isoscalar central NN-potential from chiral 3π -exchange even at next-to-leading order (considering the dominant $c_{1,2,3,4}$ -terms). For the imaginary parts of the spin-spin and tensor NN-amplitudes generated by the diagrams of class XIV one obtains the following expressions,

$$\begin{aligned} \text{Im } V_S^{(XIV)} &= \frac{g_A^4 c_4}{(4f_\pi)^6 \pi^2 \mu^3} \int_{2m_\pi}^{\mu-m_\pi} dw \sqrt{w^2 - 4m_\pi^2} \left\{ 9w^6 - 5\mu^6 - 13\mu^4 m_\pi^2 + 33\mu^2 m_\pi^4 - 15m_\pi^6 \right. \\ &\quad \left. - w^4(23\mu^2 + 37m_\pi^2) + w^2(45m_\pi^4 + 8\mu^2 m_\pi^2 + 19\mu^4) + 2m_\pi^2(\mu^2 - m_\pi^2)^3 w^{-2} \right\} \quad (19) \end{aligned}$$

$$\begin{aligned} \text{Im } V_T^{(XIV)} &= \frac{1}{\mu^2} \text{Im } V_S^{(XIV)} + \frac{2g_A^4 c_4}{(4f_\pi)^6 \pi^2 \mu^5} \int_{2m_\pi}^{\mu-m_\pi} dw \sqrt{w^2 - 4m_\pi^2} \\ &\quad \times \left\{ 9w^6 - w^4(19\mu^2 + 37m_\pi^2) + w^2(11\mu^4 + 52\mu^2 m_\pi^2 + 45m_\pi^4) \right. \\ &\quad \left. - \mu^6 - 13\mu^4 m_\pi^2 - 35\mu^2 m_\pi^4 - 15m_\pi^6 + 2m_\pi^2(m_\pi^2 - \mu^2)(\mu^4 - m_\pi^4)w^{-2} \right\}, \quad (20) \end{aligned}$$

$$\begin{aligned} \text{Im } W_S^{(XIV)} &= \frac{g_A^4}{(4f_\pi)^6 \pi^2 \mu^3} \int_{2m_\pi}^{\mu-m_\pi} dw \sqrt{w^2 - 4m_\pi^2} \lambda(w) \\ &\quad \times \left\{ -C_{13}(w) + \frac{C_2}{6} \left[w^2 + 2\mu^2 - 6m_\pi^2 + 4m_\pi^2(\mu^2 - m_\pi^2)w^{-2} \right] \right\}, \quad (21) \end{aligned}$$

$$\begin{aligned} \text{Im } W_T^{(XIV)} &= \frac{1}{\mu^2} \text{Im } W_S^{(XIII)} + \frac{g_A^4}{(4f_\pi)^6 \pi^2 \mu^5} \int_{2m_\pi}^{\mu-m_\pi} dw \sqrt{w^2 - 4m_\pi^2} \left\{ -2C_{13}(w) \right. \\ &\quad \times (m_\pi^2 + \mu^2 - w^2)^2 + \frac{C_2}{3} \left[w^6 - 4w^4(\mu^2 + 2m_\pi^2) + 2(m_\pi^2 - \mu^2)^3 \right. \\ &\quad \left. \left. + w^2(5\mu^4 + 6\mu^2 m_\pi^2 + 9m_\pi^2) + 4m_\pi^2(\mu^4 - m_\pi^4)(m_\pi^2 - \mu^2)w^{-2} \right] \right\}. \quad (22) \end{aligned}$$

This completes the presentation of analytical results. In Table 1, we present numerical results for the coordinate-space NN-potentials generated by the 3π -exchange graphs of classes X, XII, XIII and XIV for inter-nucleon distances $0.8 \text{ fm} \leq r \leq 1.4 \text{ fm}$. We use the parameters $f_\pi = 92.4 \text{ MeV}$, $m_\pi = 138 \text{ MeV}$ (average pion mass) and the central value of the nucleon axial-vector coupling-constant $g_A = 1.267 \pm 0.004$ [18]. For the second order low-energy constants $c_{1,2,3,4}$ we use the values $c_1 = -0.8 \text{ GeV}^{-1}$, $c_2 = 3.2 \text{ GeV}^{-1}$, $c_3 = -4.7 \text{ GeV}^{-1}$, $c_4 = 3.4 \text{ GeV}^{-1}$ mentioned above. One observes from Table 1 that the next-to-leading order 3π -exchange NN-potentials are often larger than the leading order ones (comparing e.g. values at $r = 1.0 \text{ fm}$). The reason for this are the large values of the low-energy constants c_3 and c_4 representing the strong Δ -excitation effects. A similar feature has also been observed for the chiral 2π -exchange NN-potential in ref.[6]. In that case the effects occurred however more selectively in the various channels. For example, there was no 2π -exchange isoscalar central potential at leading order and at next-to-leading a large isoscalar central potential with a strength of about -300 MeV at $r = 1.0 \text{ fm}$ was generated mainly by the $\pi\pi NN$ -contact vertex proportional to c_3 . Note that the low-energy constant c_3 is related to the nucleon axial polarizability [6, 13]. The repulsive isovector central potential $\widetilde{W}_C^{(XIII)}(r)$ from class XIII with a strength of almost 50 MeV at $r = 1.0 \text{ fm}$ is also fairly large. The largest potential is however the attractive isovector tensor potential $\widetilde{W}_T^{(XIII)}(r)$. At

distances $r \leq 1.1$ fm it actually overwhelms the repulsive isovector tensor potential of the (point-like) 1π -exchange. (Since the eigen-values of $\vec{\tau}_1 \cdot \vec{\tau}_2$ are -3 and $+1$ the 1π -exchange tensor potential can also act attractively, e.g. in the 3S_1 -state relevant for deuteron binding.) It is well-known that phenomenology requires a reduction of the 1π -exchange NN-tensor force at intermediate distances. The effect obtained here is presumably too strong and in addition the isovector tensor potential gets reduced by the chiral 2π -exchange (see ref.[6]). Because of the finite size (quark-substructure) of the nucleon one can trust the present calculation based on point-like chiral πN -interactions at most for distances $r \geq r_0 \simeq 1$ fm. Clearly, as soon as the nucleons start to overlap substantially the picture of an undisturbed multi-pion exchange between nucleons breaks down. The limiting distance scale $r_0 \simeq 4/m_\rho \simeq 1$ fm (with $m_\rho = 770$ MeV the ρ -meson mass) should be considered as a conservative estimate based on the argument that the nucleon axial radius $r_A \simeq \sqrt{6}/m_\rho$ receives no substantial contributions from chiral pion-loops [19]. Only by confronting chiral multi-pion exchange potentials with NN-scattering data one is able to determine this limiting distance scale r_0 more precisely.

By analyzing the elastic proton-proton scattering data-base below 350 MeV laboratory kinetic energy it has been shown recently in ref.[20] that 1π - plus chiral 2π -exchange gives a very good strong NN-force at least as far inwards as $r = 1.4$ fm (i.e. the length scale corresponding to the pion Compton wave-length $1/m_\pi$). For such distances ($r \geq 1.4$ fm) the chiral 3π -exchange NN-potential calculated here and previously in refs.[9, 10]) turns out to be a negligibly small correction. By inspection of Table 1 one observes that 3π -exchange potentials typically decrease by about a factor of 10 each 0.3 fm step outwards.

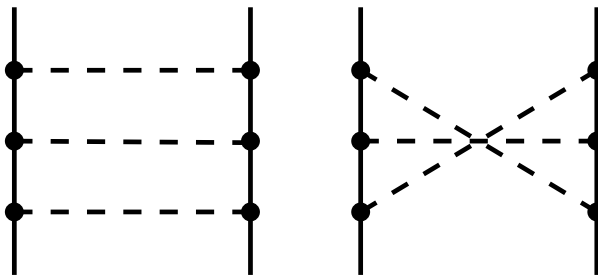


Fig.6: 3π -exchange diagrams of class VIII proportional to g_A^6 .

Finally, we like to present results for the leading order spin-spin and tensor NN-potentials generated by the 3π -exchange diagrams proportional to g_A^6 (classes VIII and IX shown in Figs.6 and 7) which could not be evaluated with the help of the spectral-function method in ref.[10]. The spin- and isospin factors of the two diagrams of class VIII (shown in Fig.6) are such that the irreducible part of the first graph and the second graph give rise only to a non-vanishing isoscalar central and isovector spin-spin and tensor potential. For the latter the spectral-function method lead to non-integrable boundary singularities in the 3π -phase space integral. Therefore an alternative calculational technique is required.

The coordinate-space potential is generally given as the 3-dimensional Fourier transform $\int d^3q \exp(i\vec{q} \cdot \vec{r}) \dots$ of the 2-loop momentum-space amplitude constructed from the propagators and vertices of a diagram. This requires in total 11 integrations, $\int d^3q d^4l_1 d^4l_2$. Usually, one performs first the integrations over the loop-energies l_{01} and l_{02} using residue calculus and one obtains this way the sum of energy denominators of all time-orderings of the diagram. In the present case this would lead to a complicated rational function of the three (on-shell) pion-energies $\omega_{1,2,3}$ which could not be further integrated analytically. The strategy is to perform a Wick-rotation of both loop-energies, $l_{0j} \rightarrow il_{4j}$, $j \in \{1, 2\}$, (of course one has to proof that this is indeed allowed) and to evaluate the remaining three 3-dimensional integrations analytically. The latter is possible because the original integrand factorizes in the variables \vec{l}_1 ,

\vec{l}_2 and $\vec{l}_3 = \vec{q} - \vec{l}_1 + \vec{l}_2$ (see also the appendix in ref.[10]). The result of this involves among other factors (originating from the vertices of the diagram) a product of three Yukawa-functions $\exp(-r\sqrt{m_\pi^2 + l_{4j}^2})/4\pi r$. This way one derives the following double-integral representations for the isovector spin-spin and tensor potentials from class VIII,

$$\begin{aligned} \widetilde{W}_S^{(VIII)}(r) &= \frac{7g_A^6}{6(16\pi f_\pi^2)^3 r^7} \left\{ e^{-3x}(8 + 18x + 16x^2 + 6x^3 + 2x^4 - x^5) \right. \\ &\quad - \int_{-\infty}^{+\infty} \frac{d\zeta_1 d\zeta_2}{\pi^2 \zeta_1 \zeta_2} \frac{\partial^2}{\partial \zeta_1 \partial \zeta_2} \left[e^{-x\Sigma} (12x^{-2} + 12x^{-1}\Sigma + 2\Sigma^2 + 8Q \right. \\ &\quad \left. \left. + x(2\Sigma Q + 6\Pi) + 2x^2\Sigma\Pi - x^4\Pi^2) \right] \right\}, \end{aligned} \quad (23)$$

$$\begin{aligned} \widetilde{W}_T^{(VIII)}(r) &= \frac{7g_A^6}{6(16\pi f_\pi^2)^3 r^7} \left\{ -e^{-3x}(1+x)(16 + 26x + 18x^2 + 6x^3 + x^4) \right. \\ &\quad + \int_{-\infty}^{+\infty} \frac{d\zeta_1 d\zeta_2}{\pi^2 \zeta_1 \zeta_2} \frac{\partial^2}{\partial \zeta_1 \partial \zeta_2} \left[e^{-x\Sigma} (36x^{-2} + 36x^{-1}\Sigma + 10\Sigma^2 + 16Q \right. \\ &\quad \left. \left. + x(10\Sigma Q + 6\Pi) + x^2(4\Sigma\Pi + 3Q^2) + 3x^3 Q\Pi + x^4\Pi^2) \right] \right\}, \end{aligned} \quad (24)$$

where we have used the dimensionless variable $x = m_\pi r$ together with various abbreviations:

$$\alpha = \sqrt{1 + \zeta_1^2}, \quad \beta = \sqrt{1 + \zeta_2^2}, \quad \gamma = \sqrt{1 + (\zeta_1 - \zeta_2)^2}, \quad (25)$$

$$\Sigma = \alpha + \beta + \gamma, \quad Q = \alpha\beta + \beta\gamma + \gamma\alpha, \quad \Pi = \alpha\beta\gamma. \quad (26)$$

The asymptotic behavior $e^{-3m_\pi r} r^{-2}$ of $\widetilde{W}_{S,T}^{(VIII)}(r)$ in eqs.(23,24) indicates that the corresponding mass-spectra start with a non-vanishing value at the 3π -threshold $\mu = 3m_\pi$. For the numerical evaluation of the principal-value integrals in eqs.(23,24) it is advantageous to employ the identity $\int_{-\infty}^{+\infty} d\zeta f(\zeta)\zeta^{-1} = \int_0^{+\infty} d\zeta [f(\zeta) - f(-\zeta)]\zeta^{-1}$, where the right hand side is singularity-free. As a check we have derived an analogous double-integral representation for the isoscalar central potential $\widetilde{V}_C^{(VIII)}(r)$ and we have found perfect agreement with the numerical results of ref.[10] based on the simpler spectral-function method.

Lastly, we come to the diagrams of class IX shown in Fig.7. For the isoscalar spin-spin and tensor NN-amplitudes the relevant sum of energy denominators is $(\omega_1^2 + \omega_2^2)/(2\omega_1^4\omega_2^4\omega_3^2)$. Since its denominator factorizes in the three variables \vec{l}_1 , \vec{l}_2 and $\vec{l}_3 = \vec{q} - \vec{l}_1 + \vec{l}_2$ one can perform the corresponding 9 integrations analytically and one gets the following closed form expressions,

$$\widetilde{V}_S^{(IX)}(r) = \frac{2g_A^6}{(16\pi f_\pi^2)^3} \frac{e^{-3x}}{r^7} (2 + 2x + x^2)(2 - 2x - 4x^2 - x^3), \quad (27)$$

$$\widetilde{V}_T^{(IX)}(r) = \frac{2g_A^6}{(16\pi f_\pi^2)^3} \frac{e^{-3x}}{r^7} (2 + 2x + x^2)(2 + x - x^2 - x^3). \quad (28)$$

We have corrected here in eq.(28) a small misprint (factor 2) which has occurred in eq.(24) of ref.[10]. The same features concerning factorization hold for the isovector central NN-amplitude and one reproduces the result $\widetilde{W}_C^{(IX)}(r) = (g_A^6/2048\pi^3 f_\pi^6 r^7) e^{-3x}(1+x)(4+5x+3x^2)$ of ref.[10]. For the isovector spin-spin and tensor potentials generated by class IX one repeats (in a slightly modified form) the technique used previously for class VIII and one ends up with the following representations,

$$\widetilde{W}_S^{(IX)}(r) = \frac{g_A^6}{3(16\pi f_\pi^2)^3 r^7} \left\{ e^{-3x}(2 + 2x + x^2)(2 - 2x - 4x^2 - x^3) - \int_{-\infty}^{+\infty} \frac{d\zeta_1 d\zeta_2}{\pi^2 \zeta_1 \zeta_2} \right.$$

$$\times \frac{\partial^2}{\partial \zeta_2^2} \left[e^{-x\Sigma} \left(12x^{-2} + 12x^{-1}\Sigma + 2\Sigma^2 + 8Q + 12\beta^2 + x((2\Sigma + 12\beta)Q - 6\Pi) \right. \right. \\ \left. \left. + x^2(2\Sigma\Pi + 4\beta^2(\alpha^2 + 3\alpha\gamma + \gamma^2)) + 4x^3(Q - \alpha\gamma)\Pi + x^4\Pi^2 \right) \right], \quad (29)$$

$$\widetilde{W}_T^{(IX)}(r) = \frac{g_A^6}{3(16\pi f_\pi^2)^3 r^7} \left\{ e^{-3x}(2 + 2x + x^2)(2 + x - x^2 - x^3) \right. \\ \left. - \int_{-\infty}^{+\infty} \frac{d\zeta_1 d\zeta_2}{\pi^2 \zeta_1 \zeta_2} \frac{\partial^2}{\partial \zeta_2^2} \left[e^{-x\Sigma} (2\Sigma^2 - 4Q + x(2\Sigma Q - 6\Pi)) \right. \right. \\ \left. \left. + x^2(Q^2 + 2\alpha^2\gamma^2) + x^3(Q + 2\alpha\gamma)\Pi + x^4\Pi^2 \right] \right\}. \quad (30)$$

Again, an analogous (double-integral) representation for the isoscalar central potential $\widetilde{V}_C^{(IX)}(r)$ turned out to be in perfect numerical agreement with the result of ref.[10] based on the spectral-function method.

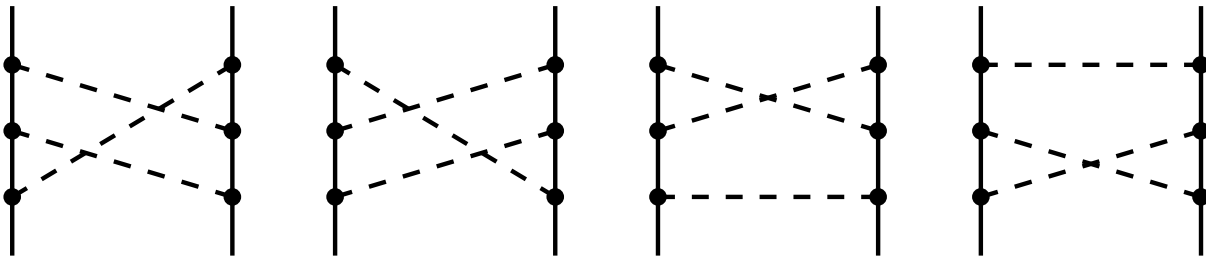


Fig.7: 3π -exchange diagrams of class IX proportional to g_A^6 .

Numerical values for the spin-spin and tensor NN-potentials generated by the diagrams of classes VIII and IX are presented in Table 1. With a typical strength of a few MeV (or less) at $r = 1.0$ fm they are comparable to the other leading order chiral 3π -exchange potentials calculated in ref.[10].

In summary, we have completed in this work the calculation of the leading order chiral 3π -exchange NN-potentials. Furthermore, we investigated the dominant next-to-leading order contributions. The (analytical) results presented here and in refs.[9, 10] are parameterfree and in a form such that they could be easily implemented in a future empirical analysis of low-energy elastic NN-scattering. This way one would be able to determine the maximal range of validity $r \geq r_0$ of chiral multi-pion exchange in the NN-interaction.

References

- [1] S. Weinberg, *Nucl. Phys.* **B363**, 3 (1991).
- [2] C. Ordonez, L. Ray and U. van Kolck, *Phys. Rev.* **C53**, 2086 (1996).
- [3] D.B. Kaplan, M.J. Savage and M.B. Wise, *Nucl. Phys.* **B534**, 329 (1998).
- [4] E. Epelbaoum, W. Glöckle and Ulf-G. Meißner, *Nucl. Phys.* **A637**, 107 (1998).
- [5] E. Epelbaoum, W. Glöckle and Ulf-G. Meißner, *Nucl. Phys.* **A671**, 295 (2000).
- [6] N. Kaiser, R. Brockmann and W. Weise, *Nucl. Phys.* **A625**, 758 (1997).
- [7] N. Kaiser, S. Gerstendörfer and W. Weise, *Nucl. Phys.* **A637**, 395 (1998).
- [8] J.C. Pupin and M.R. Robilotta, *Phys. Rev.* **C60**, 014003 (1999).
- [9] N. Kaiser, *Phys. Rev.* **C61** 014003 (2000).

r [fm]	0.8	0.9	1.0	1.1	1.2	1.3	1.4
$\widetilde{W}_S^{(X)}$ [MeV]	3.27	1.20	0.48	0.21	0.096	0.046	0.023
$\widetilde{W}_T^{(X)}$ [MeV]	-20.23	-7.33	-2.92	-1.26	-0.58	-0.28	-0.14
$\widetilde{V}_S^{(XII)}$ [MeV]	36.30	13.23	5.30	2.29	1.05	0.51	0.26
$\widetilde{V}_T^{(XII)}$ [MeV]	-18.15	-6.62	-2.65	-1.14	-0.53	-0.25	-0.13
$\widetilde{W}_S^{(XII)}$ [MeV]	17.94	6.69	2.74	1.21	0.57	0.28	0.15
$\widetilde{W}_T^{(XII)}$ [MeV]	27.02	10.00	4.07	1.78	0.83	0.41	0.21
$\widetilde{V}_C^{(XIII)}$ [MeV]	-250.0	-90.75	-36.21	-15.59	-7.14	-3.45	-1.74
$\widetilde{V}_S^{(XIII)}$ [MeV]	-112.7	-41.00	-16.39	-7.07	-3.25	-1.57	-0.79
$\widetilde{V}_T^{(XIII)}$ [MeV]	136.4	49.89	20.06	8.70	4.02	1.96	0.99
$\widetilde{W}_C^{(XIII)}$ [MeV]	333.3	121.0	48.28	20.78	9.52	4.59	2.32
$\widetilde{W}_S^{(XIII)}$ [MeV]	54.20	19.58	7.77	3.33	1.52	0.73	0.36
$\widetilde{W}_T^{(XIII)}$ [MeV]	-442.5	-162.9	-65.92	-28.79	-13.38	-6.55	-3.35
$\widetilde{V}_C^{(XIV)}$ [MeV]	250.0	90.75	36.21	15.59	7.14	3.45	1.74
$\widetilde{V}_S^{(XIV)}$ [MeV]	61.36	22.80	9.33	4.12	1.94	0.96	0.50
$\widetilde{V}_T^{(XIV)}$ [MeV]	3.13	1.40	0.66	0.33	0.17	0.089	0.049
$\widetilde{W}_S^{(XIV)}$ [MeV]	-8.78	-3.17	-1.26	-0.54	-0.24	-0.12	-0.058
$\widetilde{W}_T^{(XIV)}$ [MeV]	10.27	3.78	1.53	0.67	0.31	0.15	0.077
$\widetilde{W}_S^{(VIII)}$ [MeV]	-6.01	-2.43	-1.07	-0.502	-0.248	-0.129	-0.069
$\widetilde{W}_T^{(VIII)}$ [MeV]	15.4	6.32	2.82	1.35	0.678	0.357	0.196
$\widetilde{V}_S^{(IX)}$ [MeV]	-2.03	-1.54	-0.987	-0.607	-0.371	-0.229	-0.143
$\widetilde{V}_T^{(IX)}$ [MeV]	7.72	2.80	1.09	0.443	0.186	0.079	0.033
$\widetilde{W}_S^{(IX)}$ [MeV]	3.52	1.37	0.584	0.267	0.129	0.066	0.035
$\widetilde{W}_T^{(IX)}$ [MeV]	-0.482	-0.188	-0.079	-0.035	-0.017	-0.008	-0.004

Tab.1: Numerical values of the local NN-potentials generated by the chiral 3π -exchange graphs of classes X, XII, XIII, XIV, VIII, IX (shown in Figs. 1, 3, 4, 5, 6, 7) versus the nucleon distance r . The units of these potentials are MeV.

- [10] N. Kaiser, *Phys. Rev.* **C62** 024001 (2000).
- [11] N. Fettes, Ulf-G. Meißner and S. Steininger, *Nucl. Phys.* **A640**, 199 (1998).
- [12] P. Büttiker and Ulf-G. Meißner, *Nucl. Phys.* **A668**, 97 (2000).
- [13] V. Bernard, N. Kaiser and Ulf-G. Meißner, *Nucl. Phys.* **A615**, 483 (1997).
- [14] T.R. Hemmert, B.R. Holstein and J. Kambor, *J. Phys.* bf G34, 1831 (1998).
- [15] V. Bernard, N. Kaiser and Ulf-G. Meißner, *Nucl. Phys.* **A611**, 429 (1996).
- [16] N. Fettes, and Ulf-G. Meißner, *Nucl. Phys.* **A676**, 311 (2000).
- [17] J.L. Friar, *Phys. Rev.* **C60**, 034002 (1999).
- [18] Particle Data Group, C. Caso *et al.*, *Eur. Phys. J.* **C3**, 662 (1998).
- [19] V. Bernard, H. Fearing, T.R. Hemmert and Ulf-G. Meißner, *Nucl. Phys.* **A635**, 121 (1998).
- [20] M.C.M. Rentmeester, R.G.E. Timmermans, J.L. Friar and J.J. de Swart, *Phys. Rev. Lett.* **82**, 4992 (1999).